

Morphological Control and Photoluminescence of Zinc Oxide Nanocrystals

Tamar Andelman,[§] Yinyan Gong,[§] Mark Polking,[§] Ming Yin,[§] Igor Kuskovsky,[†] Gertrude Neumark,[§] and Stephen O'Brien^{*,§}*Department of Applied Physics and Applied Mathematics, and Materials Research Science and Engineering Center, Columbia University, New York, New York 10027, and Department of Physics, Queens College of CUNY, Flushing, New York 11367**Received: January 31, 2005; In Final Form: June 3, 2005*

Nanocrystals of the wide band gap semiconductor zinc oxide of controllable morphologies were synthesized by a simple thermal decomposition method. The predominating factor in determining the morphology (spheres, triangular prisms, and rods) was the solvent, selected on the basis of coordinating power. The nanoparticles were structurally analyzed, and the photoluminescence of each shape was compared. The intensity of the green band emission, common to many ZnO structures, was found to vary with morphology. The strongest green band intensity corresponded to the shape with the largest surface/volume ratio and could be attributed to surface oxygen vacancies. Control over the morphology of ZnO at the nanoscale is presented as a means to control the green band emission.

Introduction

The semiconductor zinc oxide, ZnO, has numerous applications, ranging from pigments and rubber additives to optoelectronic devices.^{1,2} Its wide band gap of 3.4 eV and large exciton binding energy, ~ 60 meV, make it a promising material for UV lasers.^{3,4} Various synthetic methods have been employed to create specific nanostructures, such as nanowires,^{3,5,6} nanorods,^{7,8} nanoparticles,^{9–11} nanobelts,¹² nanotetrapods,^{13,14} and more. The ability to control particle morphology is an important objective in nanocrystal synthesis, as size and shape can influence various properties.^{15,16} There have been reports of ZnO morphology control of hundreds of nanometer to micron size particles,¹⁷ and researchers have reported the elongation of particles into rods at higher precursor concentrations,⁹ but little work has been done to produce a generic simple synthetic method that is morphologically tunable on the tens of nanometer scale.^{18–20} We report here a straightforward solution method to prepare nanotriangles, a new morphology for zinc oxide, as well as nanorods and nanoparticles (spheres), by only varying solvent. The products were characterized by X-ray diffraction (XRD) and transmission electron microscopy (TEM). The effect of morphology on the photoluminescence (PL) properties is also investigated.

Experimental Section

The precursor zinc acetate dihydrate ($\text{ZnAc}_2 \cdot 2\text{H}_2\text{O}$), the capping agent oleic acid, tech. grade 90% (OA), and the solvents trioctylamine 98% (TOA), 1-hexadecanol 99% (HD), and 1-octadecene tech. grade 90% (OD) were purchased from Aldrich and used without further purification. In a standard synthesis, the precursor and capping agent in a 1:1 ratio are mixed in the solvent of choice—TOA, HD, or OD. It was found that TOA yields nanorods,⁷ HD yields nanotriangles, and OD yields spherical nanoparticles. HD with a small amount of TOA

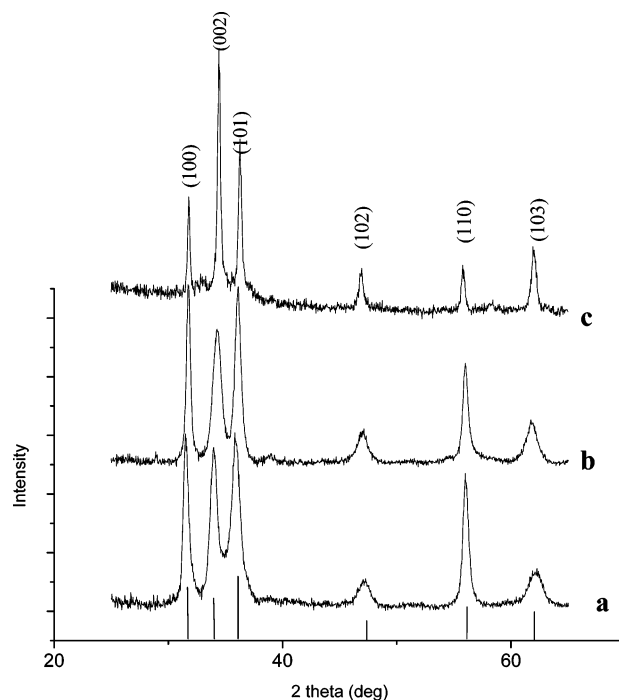


Figure 1. XRD spectra of zinc oxide (a) nanotriangles, (b) spherical nanoparticles, and (c) nanorods.

(5:1 molar ratio) was also tried to improve the triangle monodispersity, but the nanotriangles appeared the same as those without the added TOA. The mixture was then heated to 180 °C while stirring and degassed for 1 h to remove any water from the system. After the hour, the solution was heated under nitrogen to 286–300 °C. The solution turned cloudy with TOA, or white with the other solvents, when the nanocrystals formed. At this point, the heating was stopped. Upon cooling, the solution was centrifuged, and the nanoparticles were washed repeatedly and redispersed in hexane or chloroform.

The nanocrystals were characterized by XRD (Inel Multi-purpose diffractometer) and TEM (JEOL 100cx). For XRD, the nanocrystal solution was drop cast onto a silicon wafer, and

* Author to whom correspondence should be addressed. E-mail: so188@columbia.edu.

[§] Columbia University.

[†] Queens College of CUNY.

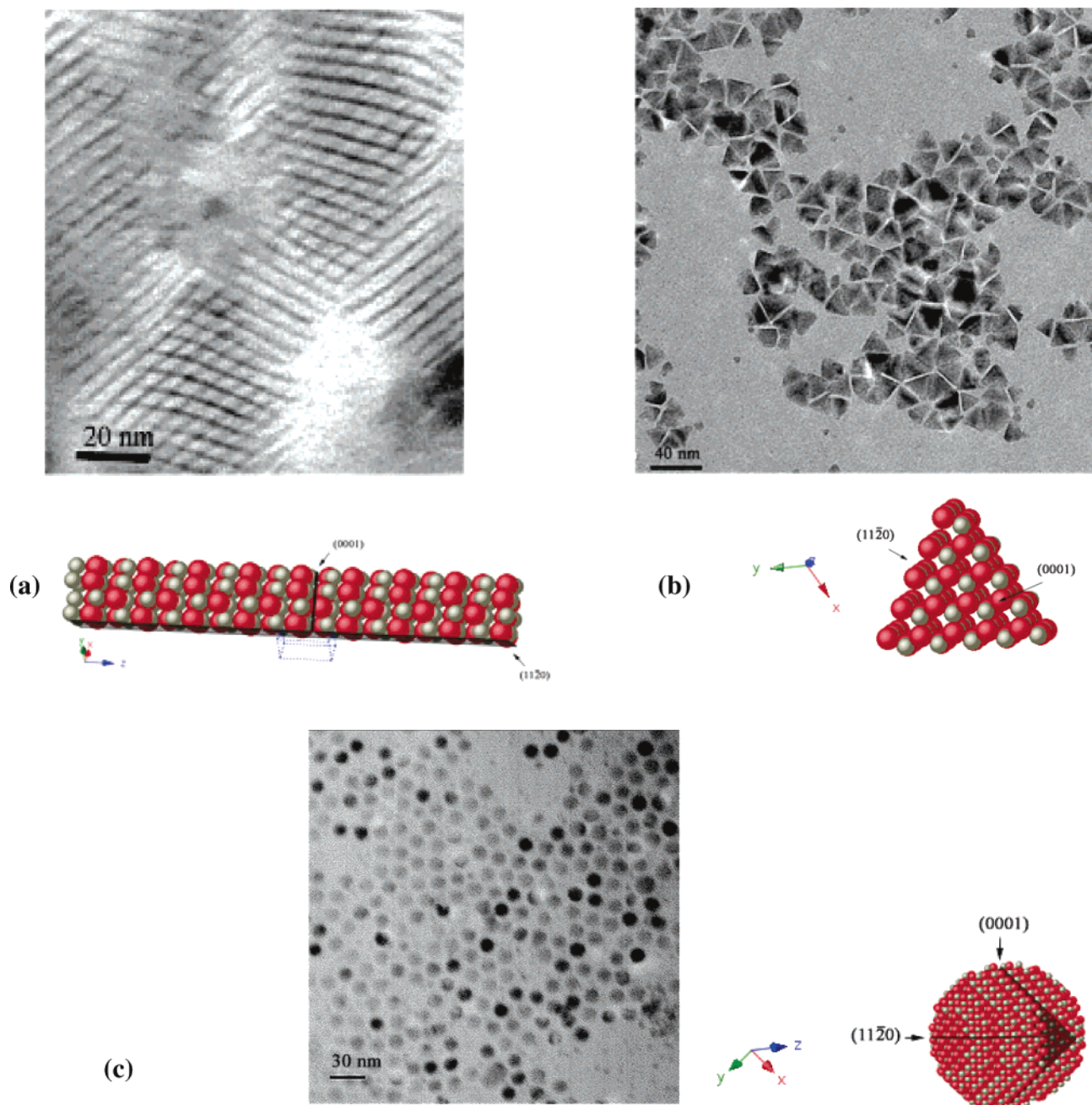


Figure 2. TEM images of zinc oxide with a corresponding representative model (a) nanorods, prepared in TOA, (b) nanotriangles (triangular prisms), prepared in HD, and (c) spherical nanoparticles, prepared in OD.

the XRD spectrum was recorded. For TEM, a drop of the nanocrystal solution was placed on a 400 mesh carbon grid with Formvar. Photoluminescence (PL) spectroscopy was performed at room temperature (RT), using the 325 nm emission from a He–Cd laser (the maximum excitation intensity, $I_{\max} \approx 28$ W/cm²). Neutral density filters were used to change the excitation intensity. The solution with nanocrystal was kept in a quartz cell.

Results and Discussion

The XRD pattern of each nanocrystal shape matches the standard bulk wurtzite structure (*P63mc*, JCPDF No. 36-1451), as shown in Figure 1. The intensity of the peaks in the nanorod sample differs from the bulk due to the larger number of planes along the long axis of the rod as compared to the diameter.⁷ The relative intensity of the peaks in the XRD spectra of the

nanotriangles and spherical nanoparticles matches the bulk, signifying no preferred orientation. This seems to indicate that the nanotriangles are not thin plates, which would give rise to preferred orientation for reasons similar to the nanorods, but more like prisms or pyramids. The triangular samples prepared with TOA and without yielded the same XRD spectra.

TEM images of the prepared samples are shown in Figure 2. In Figure 2a, the sample prepared in trioctylamine (TOA) shows nanorods, which self-assemble into stacks and have a diameter of 2 nm and lengths ranging from 40 to 50 nm. Figure 2b shows the sample prepared in hexadecanol (hexadecanol with a small amount of TOA produced the same result), which yielded nanotriangles with a side length ranging from 13 to 21 nm. Note the tendency to self-assemble. This unique shape might provide for interesting superstructures. Figure 2c shows the spherical nanoparticles prepared from octadecene (OD) with a diameter

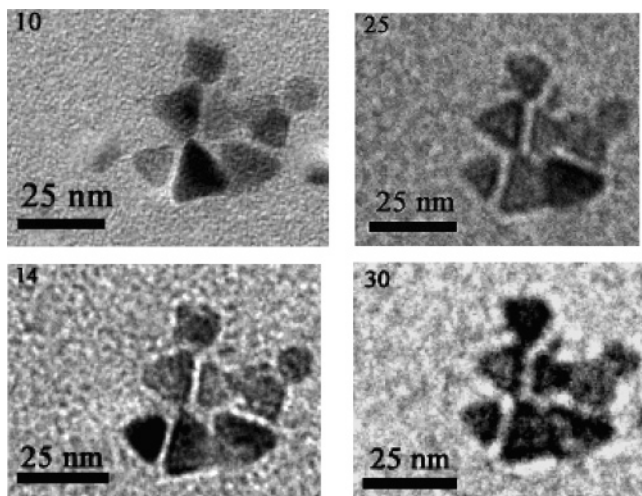


Figure 3. TEM images of ZnO nanotriangles at various degrees of tilt. The degree of tilt is indicated in the top left-hand corner. At all angles, the shape remains triangular.

range of 12–14 nm. Below each TEM picture appears a corresponding model, with planes labeled. The triangular model represents the likeliest structure for the shape. Tilting experiments (Figure 3) were performed to determine the three-dimensional shape of the nanotriangles. Retention of the triangular shape gives evidence in favor of the equilateral triangle shape over the pyramidal shape for the three-dimensional morphology.^{21,22}

The nature of the solvents and the particle growth in the solvents can be used to explain why each solvent gives rise to its particular morphology. Crystal morphology is determined by the relative growth rates of the crystal planes, which can differ greatly due to differences in surface free energies.^{23,24} It has been reported that varying the capping agent or ratio of capping agent to precursor has changed particle morphology in a number of systems, due to the varying ability to stabilize certain planes.^{25–27} In our system, the ratio of capping agent to precursor was held constant, and the solvent was changed, indicating that the different solvents play significant roles in stabilizing specific crystallographic planes of the growing nanocrystal. A common synthetic method for rod formation is to use two different capping ligands that selectively bind to different planes, thus creating a difference in surface energies between planes and encouraging growth along one direction.²⁷ We found that nanorods formed in the presence of trioctylamine (TOA) and oleic acid. It is believed that trioctylamine is a relatively strong coordinating solvent and can also act as a ligand. Thus, it is most likely the combination of the two ligands (TOA and oleic acid) that supports rod growth, with growth parallel to the rod axis greatly inhibited by ligand binding to the surface corresponding to the {11-20} plane and other planes commensurate with this geometry. When the solvent was switched from trioctylamine to octadecene, spherical nanoparticles formed. Octadecene is not a coordinating solvent, so no one crystal plane was favored as a growth direction. It seems that, as a result of this, the particles grow in a spherical shape, which minimizes surface area.²⁷ The last solvent selected, hexadecanol, is a moderately coordinating solvent and can be thought of as a relatively weak ligand. Unlike the rods, growth in all but one direction is not inhibited. Nevertheless, we surmise that the combination of oleic acid and the mild coordinating power of the solvent result in growth along preferred planes, giving rise to the faceting required for nanotriangle growth.

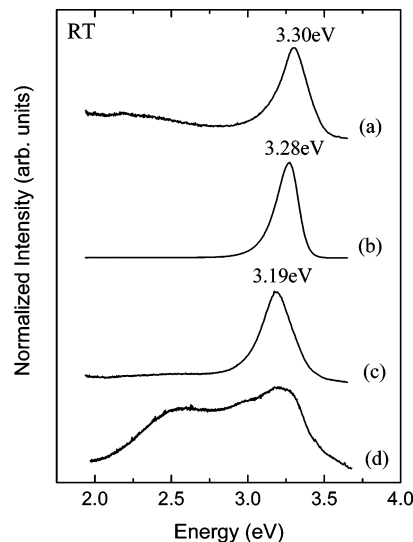


Figure 4. The RT PL spectra of ZnO (a) nanotriangles synthesized in pure hexadecanol, (b) nanotriangles prepared from TOA/hexadecanol, (c) spherical nanoparticles, and (d) nanorods.

The room temperature (RT) PL spectra of nanotriangles and spherical nanoparticles obtained using the maximum excitation in this experiment are shown in Figure 4 (the RT PL spectrum of nanorods^{7,28} is also plotted in Figure 5 for comparison). In all cases, the PL is dominated by the near-band-edge UV emission (3.30 and 3.19 eV for nanotriangles and spherical nanoparticles, respectively). No peak energy shifts were observed upon varying the excitation intensity by about 2 orders of magnitude (see Figure 5a,b). Although no structural difference between nanotriangles synthesized in just hexadecanol and those formed in TOA/hexadecanol was observed in the XRD or TEM, in the PL spectra, a difference is evident. The origin of the UV peak in these nanocrystallites is not well understood and can be attributed to either excitonic or defect-related emission and might depend on the synthesis method.²⁹ Here, we observe that the UV peak for spherical nanocrystals is comparatively redshifted by about 200 meV and, thus, might be due to surface defects.²⁹ In addition to the UV peak, the spectrum of the nanotriangles synthesized from only hexadecanol reveals a weak broad green emission, while the nanotriangles synthesized from TOA/hexadecanol and the spherical nanoparticles do not exhibit any significant luminescence in this spectral region. The nanorods, however, exhibit a large broad green band. For further comparison, we note that the green PL of nanotriangles from pure hexadecanol becomes more pronounced at lower excitation intensities, and its intensity grows comparable with that of the UV peak (Figure 5a). On the contrary, for the nanotriangles synthesized from TOA/hexadecanol and the spherical nanoparticles, no significant green emission can be observed even at the lowest excitation intensity (Figure 5b).

It has been suggested that the green band emission is due to deep levels, far from the valence or conduction band edge, associated with various types of oxygen vacancies in ZnO,^{30–38} and that photogenerated holes participate in such a recombination.²⁸ The photoluminescence due to the deep levels becomes more pronounced with decreasing excitation as the quasi-Fermi levels move toward the mid-gap, and it should ultimately dominate if concentration of such defects is sufficiently high. It is known in the case of semiconductor nanocrystals that single crystal annealing temperatures are suppressed (it is relatively easy to grow a single crystal of a few nanometers in this temperature range), and that it is believed a majority of defects lie at the surface or interface with the ligand capping groups

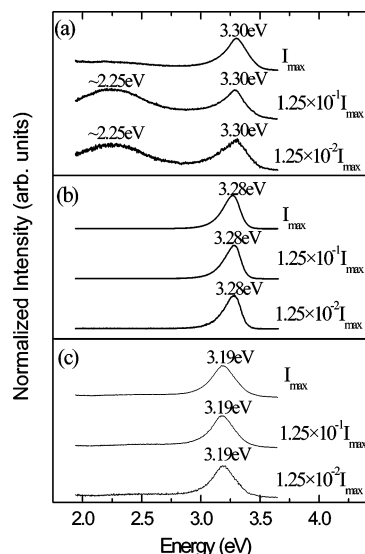


Figure 5. RT PL spectra at different excitation intensities (a) nanotriangles from pure HD, (b) nanotriangles from TOA/hexadecanol, and (c) spherical nanoparticles.

that have arrested growth. To evaluate contributions to the emission spectra as a function of nanocrystal morphology, we make the assumption that surface defects play a significant role. A calculation of the aspect ratio of each nanoparticle shape reveals that nanorods, with their extremely small diameter, have the largest surface area-to-volume ratio. Due to size, the spherical nanoparticles have the lowest ratio, and the nanotriangles fall in between. Correspondingly, the intensity of the green band for each morphology follows the same order; the nanorods have the strongest green band, the nanotriangles in pure hexadecanol have mild green emission, and the spherical nanoparticles have none. Thus, our results suggest that the green band is due to radiative recombination between free holes and the donor surface states, and therefore, the nanoparticle shapes with larger surface area/volume ratios (more surface than inside) will exhibit stronger green band emission. The exact origin of the green band observed in ZnO is still controversial, and, at least, in nanocrystals, its origin can depend on the fabrication technique.³⁹ While the bulk origin of the green PL cannot be completely disregarded, recently, Harada and Hashimoto⁴⁰ have presented strong evidence that the green band even in bulk ZnO might originate from the surface states, supporting our results.

Oxygen vacancies (as mentioned above) are the most often suggested defects.^{30–38} We believe that the absence of the green band in the PL from the nanotriangles synthesized in TOA/hexadecanol supports this assumption. It is possible that TOA removes the hydrogen from the oleic acid (deprotonation), leaving a characteristic carboxylate anionic headgroup, which then allows the oleic acid to behave as a bidentate ligand, coordinating to Zn^{2+} , and filling any surface oxygen vacancies. One might postulate that this would then result in nanotriangles with much fewer surface oxygen vacancies and, therefore, no green band. However, the nanorods are also synthesized in TOA, and do exhibit a broad green band. In this system, TOA is the only solvent (unlike the case of the nanotriangles, in which HD is the primary solvent), plus the resulting product (rods) has a significantly larger surface area/volume ratio (rod diameter is ~ 2 nm), which may mean, given so many of the atoms are at the surface, that oxygen vacancies cannot be compensated for. Direct comparisons between the photoluminescence of the triangle and spheres are reasonable because of the similarities between surface area/volume ratios and the synthesis methods

employed, whereas it is harder to make the same comparison with the rods. The behavior of the two different solvent/ligand systems, TOA/oleic acid and TOA/HD/oleic acid, and the respective products remain an interesting subject for further investigation.

Conclusion

In conclusion, we have developed a straightforward synthetic procedure to prepare zinc oxide nanocrystals of controllable morphology (spheres, rods, and triangular prisms) by selection of solvent. The nanotriangle shape, observed in other systems, is a novel shape for zinc oxide. The nanocrystals remain ligand-capped, are easily dispersed in hydrocarbon solvents, and show a tendency to self-assemble upon evaporation onto substrates. Photoluminescence measurements indicated that the green band emission is associated with surface defects and shows a strong dependence on morphology, with suppression of the green band emission in the case of spherical nanoparticles (prepared in octadecene) and nanotriangles prepared in TOA/hexadecanol.

Acknowledgment. The authors gratefully acknowledge financial support of this work primarily by the National Science Foundation under CAREER DMR-0348938, in part by the Department of Energy, Office of Basic Energy Sciences, Catalysis Futures Grant DE-FG02-03ER15463, and in part by the NSF MRSEC program DMR-0213574. The authors thank Dr. Elena Schevchenko for her helpful advice. T.A. is grateful for support from the NDSEG Fellowship Program.

References and Notes

- Lee, C. J.; Lee, T. J.; Lyu, S. C.; Zhang, Y.; Ruh, H.; Lee, H. J. *Appl. Phys. Lett.* **2002**, *81*, 3648.
- Xu, C. X.; Sun, X. W.; Chen, B. J.; Shum, P.; Li, S.; Hu, X. J. *Appl. Phys.* **2004**, *95*, 661.
- Huang, M. H.; Mao, S.; Feick, H.; Yan, H.; Wu, Y.; Kind, H.; Weber, E.; Russo, R.; Yang, P. *Science* **2001**, *292*, 1897.
- Johnson, J. C.; Yan, H.; Schaller, R. D.; Haber, L. H.; Saykally, R. J.; Yang, P. *J. Phys. Chem. B* **2001**, *105*, 11387.
- Lyu, S. C.; Zhang, Y.; Lee, C. J.; Ruh, H.; Lee, H. J. *Chem. Mater.* **2003**, *15*, 3294.
- Li, Y.; Meng, G. W.; Zhang, L. D.; Philipp, F. *Appl. Phys. Lett.* **2000**, *76*, 2011.
- Yin, M.; Gu, Y.; Kuskovsky, I.; Andelman, T.; Zhu, Y.; Neumark, G. F.; O'Brien, S. J. *Am. Chem. Soc.* **2004**, *126*, 6206.
- Li, J. Y.; Chen, X. L.; Li, H.; He, M.; Qiao, Z. Y. *J. Cryst. Growth* **2001**, *233*, 5.
- Guo, L.; Yang, S.; Yang, C.; Yu, P.; Wang, J.; Ge, W.; Wong, G. *Chem. Mater.* **2000**, *12*, 2268.
- Meulenkamp, E. *J. Phys. Chem. B* **1998**, *102*, 5566.
- Cozzoli, P.; Curri, M.; Agostiano, A.; Leo, G.; Lomascolo, M. *J. Phys. Chem. B* **2003**, *107*, 4756.
- Pan, Z.; Dai, Z. R.; Wang, Z. L. *Science* **2001**, *291*, 1947.
- Chen, Z.; Shan, Z.; Cao, M.; Lu, L.; Mao, S. *Nanotechnology* **2004**, *15*, 365.
- Yan, H.; He, R.; Pham, J.; Yang, P. *Adv. Mater.* **2003**, *15*, 403.
- Alivisatos, A. P. *Science* **1996**, *271*, 933.
- Lieber, C. *Solid State Commun.* **1998**, *107*, 607.
- Zhang, J.; Sun, L.; Yin, J.; Su, H.; Liao, C.; Yan, C. *Chem. Mater.* **2002**, *14*, 4172.
- Zhang, J.; Sun, L.; Jiang, X.; Liao, C.; Yan, C. *Cryst. Growth Des.* **2004**, *4*, 309.
- Wang, L.; Muhammed, M. *J. Mater. Chem.* **1999**, *9*, 2871.
- Yan, H.; He, R.; Pham, J.; Yang, P. *Adv. Mater.* **2003**, *15*, 402.
- Pinna, N.; Weiss, K.; Urban, J.; Pileni, M. *Adv. Mater.* **2001**, *13*, 261.
- Pinna, N.; Weiss, K.; Sack-Kongehl, H.; Vogel, W.; Urban, J.; Pileni, M. *Langmuir* **2001**, *17*, 7982.
- Pacholski, C.; Kornowski, A.; Weller, H. *Angew. Chem., Int. Ed.* **2002**, *41*, 1188.
- Cozzoli, P. D.; Kornowski, A.; Weller, H. *J. Am. Chem. Soc.* **2003**, *125*, 14539.
- Sau, T.; Murphy, C. *J. Am. Chem. Soc.* **2004**, *126*, 8648.
- Herricks, T.; Chen, J.; Xia, Y. *Nano Lett.* **2004**, *4*, 2367.

- (27) Manna, L.; Scher, E.; Alivisatos, P. *J. Am. Chem. Soc.* **2002**, *122*, 12700.
- (28) Gu, Y.; Kuskovsky, I. L.; Yin, M.; O'Brien, S.; Neumark, G. F. *Appl. Phys. Lett.* **2004**, *85*, 1.
- (29) Fonoberov, V. A.; Balandin, A. A. *Appl. Phys. Lett.* **2004**, *85*, 5971.
- (30) Lin, B.; Fu, Z.; Jia, Y. *Appl. Phys. Lett.* **2001**, *79*, 943.
- (31) Kroger, F. A.; Vink, H. J. *J. Chem. Phys.* **1954**, *22*, 250.
- (32) Kasai, P. H. *Phys. Rev.* **1963**, *130*, 989.
- (33) Vanheusden, K.; Seager, C. H.; Warren, W. L.; Tallant, D. R.; Voigt, J. A. *Appl. Phys. Lett.* **1996**, *68*, 403.
- (34) Vanheusden, K.; Warren, W. L.; Seager, C. H.; Tallant, D. R.; Voigt, J. A.; Gnade, B. E. *J. Appl. Phys.* **1996**, *79*, 7983.
- (35) Liu, M.; Kitai, A. H.; Mascher, P. *J. Lumin.* **1992**, *54*, 35.
- (36) Reynolds, D. C.; Look, S. C.; Jogai, B.; Morkoc, H. *Solid State Commun.* **1997**, *101*, 643.
- (37) Reynolds, D. C.; Look, S. C.; Jogai, B. *J. Appl. Phys.* **2001**, *89*, 6189.
- (38) Garces, N. Y.; Wang, L.; Bai, L.; Giles, N. C.; Halliburton, L. E.; Cantwell, G. *Appl. Phys. Lett.* **2002**, *81*, 622.
- (39) Li, D.; Leung, H.; Djurišić, A. B.; Liu, Z. T.; Xie, M. H.; Shi, S. L.; Xu, S. J.; Chan, W. K. *Appl. Phys. Lett.* **2004**, *85*, 1601.
- (40) Harada, Y.; Hashimoto, S. *Phys. Rev. B* **2003**, *68*, 045421.